ISSN 0010-5082, Combustion, Explosion, and Shock Waves, 2018, Vol. 54, No. 5, pp. 606–613. © Pleiades Publishing, Ltd., 2018.
Original Russian Text © K.A. Ten, E.R. Pruuel, A.O. Kashkarov, I.A. Rubtsov, M.V. Antipov, A.B. Georgievskaya, A.L. Mikhailov, I.A. Spirin, V.M. Aulchenko, L.I. Shekhtman, V.V. Zhulanov, B.P. Tolochko.

Detection of Particle Ejection from Shock-Loaded Metals by Synchrotron Radiation Methods

K. A. Ten[a], E. R. Pruuel[a], A. O. Kashkarov[a], I. A. Rubtsov[a,e], M. V. Antipov[b], A. B. Georgievskaya[b], A. L. Mikhailov[b], I. A. Spirin[b], V. M. Aulchenko[c], L. I. Shekhtman[c], V. V. Zhulanov[c], and B. P. Tolochko[d]

UDC 532.529.+533.6

Published in *Fizika Goreniya i Vzryva*, Vol. 54, No. 5, pp. 103–111, September–October, 2018.
Original article submitted March 21, 2018.

Abstract: The mass distribution along a flow of microparticles is measured by methods of synchrotron radiation generated by the VEPP-3 collider. The use of the soft spectrum of radiation allows microparticle flows to be measured with a record-beating (minimum) specific density (1 mg/cm^3). Simultaneous recording of microparticle flows by piezoelectric sensors offers a possibility of comparisons and extension of results.

Keywords: shock wave, free surface, particle ejection, synchrotron radiation, x-ray detector.

DOI: 10.1134/S0010508218050143

INTRODUCTION

Investigations of shock wave loading of various materials revealed the effect known as particle ejection [1]. The essence of this phenomenon implies the formation of a region (flow) of micro- and nanoparticles when a strong shock wave reaches the free surface (FS). Spalling fracture at the FS boundary occurs under the action of high (both tensile and compressive) stresses induced by interaction of incident and reflected shock waves. The situation is aggravated by the fact that the matter interface (i.e., FS) is not flat (there are roughness elements ranging from 1 to 100 μm on this surface). Therefore, the dynamics of a cloud of microparticles of the disperse phase of matter in high-speed gas-dynamic processes is a complicated problem from both scientific and engineering viewpoints.

The first investigations of these processes were started at the Institute of Experimental Physics in the 1960s, but the first results were published only in 1998 [2]. Later on, such investigations were performed at the Institute of Experimental Physics [1–4] and Los Alamos National Laboratory [5–8]. It was found that the flow of microparticles from the cloud is significantly affected by the FS roughness and the ejected mass is proportional to the roughness amplitude (Rz). Today this phenomenon is still not adequately studied, and the experimental techniques are far from being perfect.

In recent years, the interest to the particle ejection phenomenon was revived [1] owing to qualitative improvement of experimental techniques, such as laser methods [5, 6, 9–11], optical methods [4, 6], measurements by piezoelectric sensors [12, 13], and x-ray diffraction analysis [1, 14]. In addition, principally new methods of research with the use of high-energy accelerators were developed: proton beams [15] and synchrotron radiation [16–18]. The increasing interest to particle ejec-

[a] Lavrentyev Institute of Hydrodynamics, Siberian Branch, Russian Academy of Sciences, Novosibirsk, 630090 Russia; ten@hydro.nsc.ru.
[b] Institute of Experimental Physics (VNIIEF), Russian Federal Nuclear Center, Sarov, 607188 Russia.
[c] Budker Institute of Nuclear Physics, Siberian Branch, Russian Academy of Sciences, Novosibirsk, 630090 Russia.
[d] Institute of Solid State Chemistry and Mechanochemistry, Siberian Branch, Russian Academy of Sciences, Novosibirsk, 630158 Russia.
[e] Novosibirsk State University, Novosibirsk, 630090 Russia.

tion is also closely related to the influence of dust ejection from the FS on the measurements of its dynamics by shadowgraphy, electric contact and laser methods; moreover, this phenomenon plays an important role in some physical processes, for example, in inertial thermonuclear fusion with plasma confinement [19].

In one group of studies of the particle ejection process, it is assumed that the main source of the dust cloud is the development of the Richtmyer–Meshkov instability in the metal (or liquid). Periodic perturbations of various amplitudes are applied to the FS in experiments [1, 20–23]. The goal of such activities is to find the effects of perturbations on the metal surface and the amplitude and shape of the shock wave on the distribution of the density of matter ejected into the ambient space, the mass of this matter, the particle velocity, and the particle size distribution.

One of the promising directions of studying the disperse phase dynamics in high-speed processes is detection of particle motion by the method of heterodyne laser interferometry or photon Doppler velocimetry (PDV); however, interpretation of recorded data is rather difficult at the moment. To facilitate the data interpretation, it is possible to measure flows of particles whose size, mass, and shape factor are known. In such experiments, a layer of calibrated particles is deposited onto the FS of the flyer plate, followed by shock wave loading of the plate and acceleration of disperse phase particles. Comparisons of experimental data with numerical predictions allow one to verify the validity of numerical models and to obtain data on the dynamics of motion of particles with known parameters. These data can be compared with the results measured during the process of particle ejection, where the particle parameters are not known in advance [24].

The majority of experimental investigations are aimed at studying the influence of the shape and size of periodic inhomogeneities (pits or grooves) on the metal surface on particle ejection [25–27]. The existing methods of particle detection (optical, XRD, and laser methods) allow determination of the maximum particle velocity and particle momentum (piezoelectric sensors) and microparticle size (optical and holographic sensors [11]). The greatest problem in all methods is to determine the mass distribution along the particle flow (especially in the field of low densities from 1 to 100 mg/cm^3).

In the present work, the particle flow from the metal FS was measured with the use of synchrotron radiation (SR) generated by the VEPP-3 accelerator developed at the Budker Institute of Nuclear Physics, Siberian Branch, Russian Academy of Sciences (Novosibirsk) [28]. Synchrotron radiation generated by VEPP-3 has a soft x-ray spectrum (8–30 keV), identical short pulses (shorter than 1 ns), and small divergence (less than 0.5 mrad), which ensures detection of particle flows with very low densities [29, 30]. The high repeatability of SR pulses ensures accurate calibration of the DIMEX detector before and after the explosion experiment [31, 32]. The high accuracy of detector calibration makes it possible to determine the distribution of the specific mass of the particle flow along the trajectory of particle motion. The microparticle flow with the use of SR was visualized simultaneously with measurements performed by piezoelectric sensors. Piezoelectric sensors found many applications owing to the simplicity of obtaining information on dynamic flows of microparticles [12]. The main drawback of this method is the problem of dynamic calibration of piezoelectric sensors. It is desirable to use these sensors together with other methods, which allow one to estimate the particle mass and flow velocity. Synchrotron radiation is an ideal supplement to piezoelectric sensors. Comparing the data on the microparticle flow (velocity and particle mass) with the signal detected by the piezoelectric sensor, one can perform independent calibration of sensor readings.

We studied flows of microparticles from grooves (roughness elements) 6–60 μm on the tin surface. The mass distributions along the microparticle flow obtained in the study are found to be in good agreement with the calculations performed at the Institute of Experimental Physics [1, 14]. These data are needed for numerical simulation of the particle ejection processes.

ARRANGEMENT OF EXPERIMENTS

The experiments were performed at the station entitled "Extreme state of matter" at the VEPP-3 collider. The electron energy was 2 GeV, and the SR spectrum of a three-pole wiggler was in the interval from 8 to 30 keV [28, 30]. Synchrotron radiation was formed by a collimator shaped as a band 20 mm wide and 0.2 mm high. The position of the FS of the tin disk with grooves and the detector with respect to the SR beam is shown in Fig. 1. The disk accelerated by an explosion moves along the DIMEX detector [31], across the SR beam. The recording part of the detector consists of channels with the size 0.1 × 1.0 × 30 mm (width, height, and depth, respectively). There are 512 channels in the detector, i.e., the recording zone length is 51 mm, and the linear resolution is 0.1 mm. Copper foil 15, 30, and 50 μm was used for calibration. In the experiments, the DIMEX detector measured the distribution of transmitted SR, which was used as a basis for calculating the distribution of the linear mass (amount of matter along

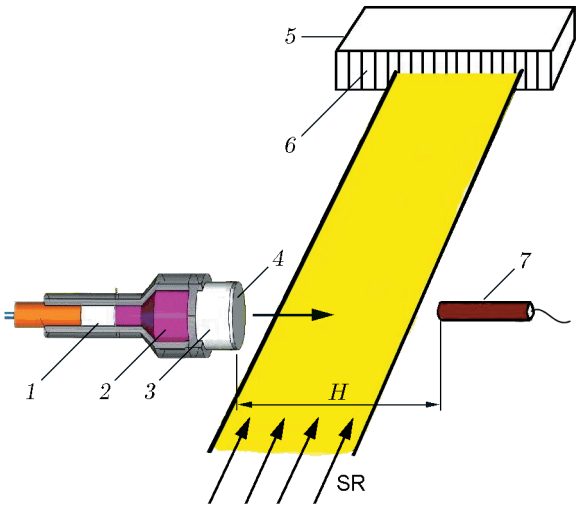

Fig. 1. Positions of the specimen, detector, and SR plane in experiments aimed at longitudinal registration of the mass distribution of the microparticle flow: (*1*) intermediate HE charge; (*2*) explosive lens; (*3*) main HE charge; (*4*) examined specimen (tin disk); (*5*) DIMEX detector; (*6*) detector channels; (*7*) piezoelectric sensor.

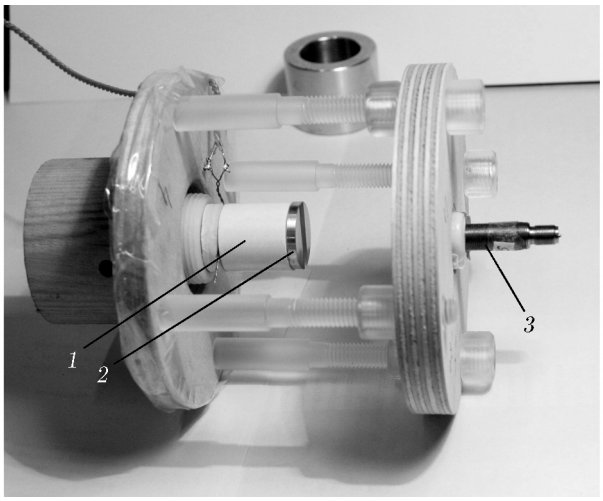

Fig. 2. General view of the experimental setup for shock loading of the specimen with the use of SR: (*1*) HE charge; (*2*) tin plate; (*3*) piezoelectric sensor.

the SR beam ρd [g · cm^2]) along the detector. The linear mass distribution (512 channels, which form one frame) was recorded with a step of 0.5 μs and exposure time of 1 ns. The DIMEX detector can write down 32 frames.

A photograph of the experimental setup is shown in Fig. 2. The tin disk was accelerated by an explosion of a pressed HMX pellet 20 mm in diameter and 20 mm

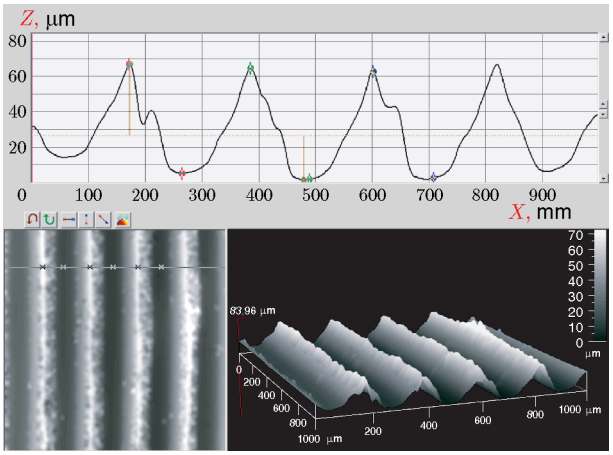

Fig. 3. Profile of grooves on the free surface.

long. The charge was initiated by an explosive lens via an intermediate HMX charge. The total mass of the HE assembly (together with the detonator) was within 12 g. The explosive setup was placed into a chamber, which was evacuated before the experiment to a pressure of 0.01 atm. Some of the experiments were performed at the atmospheric initial pressure. In all experiments, the detector and the oscillograph recording the piezoelectric sensor signal were triggered by a wire transducer located in the explosive lens. The piezoelectric sensor 7 [12] recorded the pressure of the impinging dusty flow. The sensor (with the tip diameter of 5 mm) was located at a distance H = 18, 28, or 62 mm from the FS (see the table).

The FS of the tin specimen was milled to apply surface roughness, which was varied from one experiment to another. The rough surface was formed by grooves of depth A aligned with a step λ. Figure 3 shows the measured profile of the grooves on the specimen. The roughness area was a band of width L, whereas the remaining part of the FS was polished. The thickness of all tin specimens was 3 mm, and their diameter was 20 mm. The groove parameters A, λ, and L used in the present experiments are summarized in the table.

As the length of the SR detection region (≈20 mm) in some experiments was smaller than the distance from the FS to the piezoelectric sensor, the experiments were arranged in two ways. In variant 1, the detector registered the initial FS motion, dust cloud formation, and time instant of the impact (interaction of the dust cloud with the piezoelectric sensor). In variant 2 (with large distances from the sensor), the field of vision of the detector captured either the initial stage of dust cloud formation, or the instant of the impact onto the piezoelectric sensor.

Initial data in experiments

Roughness Rz, μm	FS profile parameters			H, mm	Pressure in the explosive chamber, atm
	A, μm	λ, μm	L, mm		
6	6	50	20	18, 62	0.01, 1.0
60	60	250	5	18, 28	0.01, 1.0

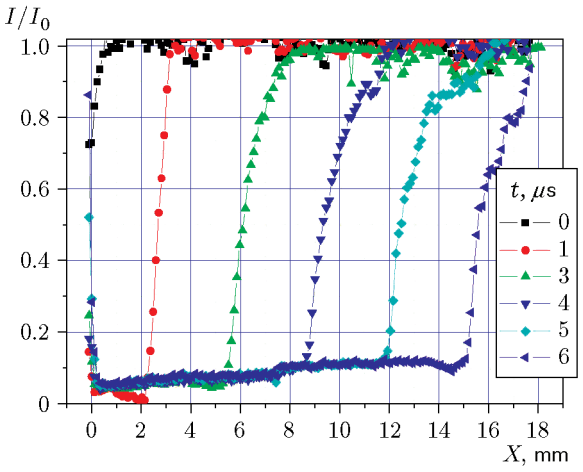

Fig. 4. Record of the normalized SR intensity in the first frames taken by the detector (the frame numbers correspond to the number of microseconds after the beginning of disk motion).

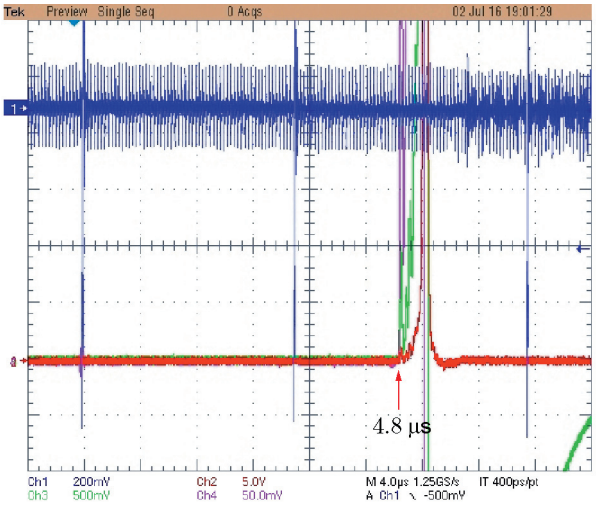

Fig. 5. Oscillogram of the signal recorded by the piezoelectric sensor (the time is counted from the beginning of disk motion).

EXPERIMENTAL RESULTS

The results for two variants of experimental arrangement are described below.

Variant 1 ($Rz = 6$ μm, $A_0/\lambda/L = 6/50/20$)

In these experiments, the frames in the detector (one frame means registration of the distribution of transmitted radiation in the flow motion direction) were taken with an interval of 1 μs; therefore, for a convenient presentation of the oscillograms and detector frames, the frame numbers correspond to the number of microseconds from the beginning of FS (disk) motion. Figure 4 shows the record of the DIMEX detector signal, where frame No. 17 is chosen as a zero time instant [the FS (disk) motion starts in this frame]. This frame is denoted by $t = 0$. Correspondingly, the beginning of signal growth ($t = 4.8$ μs) on the oscillogram (Fig. 5) is counted from the same time instant.

Figure 6 shows the X–t diagram of the flow and FS (disk) positions (the time is counted from the beginning of disk motion). The X coordinate is counted from the initial FS (disk) position. The piezoelectric sensor is located at a distance of 18 mm from the disk. The initial velocities of the particle flow and the disk are 3.86 and 2.8 km/s, which agrees well with the predicted data. The flow of the dust cloud (jet) reaches the sensor at the 5th microsecond, which is consistent with the sensor reading on the oscillogram (see Fig. 5).

Figure 7 shows the distribution of the linear mass at the first microseconds after the beginning of FS motion. Detector absorption was calibrated on copper foil and recalculated for tin. The visible mass distribution is nonuniform and time-dependent.

Variant 2 ($Rz = 60$ μm, $A_0/\lambda/L = 60/250/5$)

The sensor is located at a distance of 28 mm from the FS. The jet reaches the sensor in 7 μs, while the FS reached the sensor in 11 μs, which coincides with the oscillogram in Fig. 8. The sensor started to write the signal in 6.8 μs. Further, after 4.0 μs, the signal exhibits a drastic increase. Here the time is also counted from the beginning of FS (disk) motion.

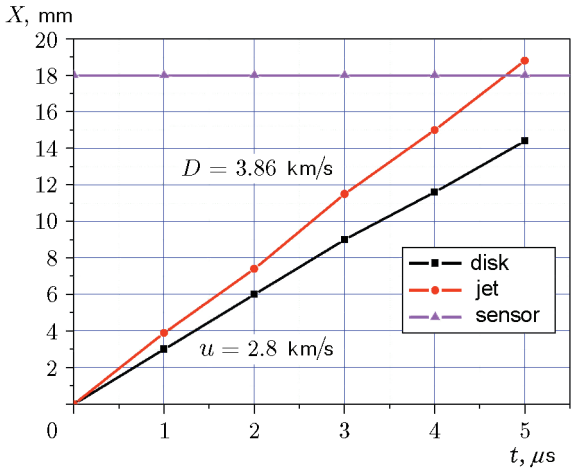

Fig. 6. Calculated positions of the disk, jet, and sensor [X is the distance counted from the initial position of the disk (FS)].

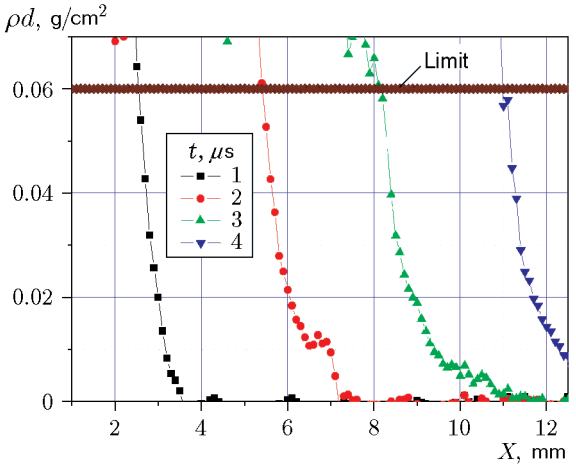

Fig. 7. Distribution of the specific mass on the SR beam in time.

Figure 9 shows the frames taken by the DIMEX detector: normalized distributions of transmitted SR. At the time $t = 7$ μs, the jet reaches the piezoelectric sensor, and the disk impinges on the sensor at $t = 11$ μs. The X–t diagram of the jet and FS (disk) positions is shown in Fig. 10.

Joint recording of the piezoelectric sensor and x-ray radiography allowed us to obtain the distribution of the jet mass at the time instants $t = 7$ μs (when the jet reaches the sensor) and $t = 11$ μs (at the instant of the FS impact onto the sensor). They are presented in Fig. 11 together with the calculation errors (thin lines). The limit of measurement calibration is also indicated. The total mass of the jet (from 18 to 28 mm in Fig. 11) is 5.6 mg/cm^2, which agrees with the data of [14] (3.9–8 mg/cm^2).

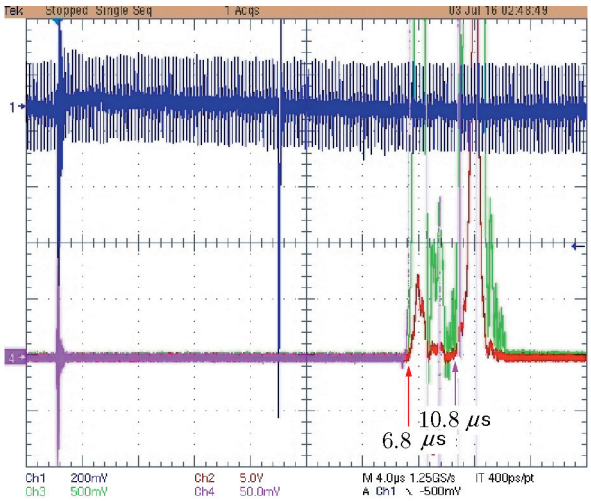

Fig. 8. Oscillogram of the signal recorded by the piezoelectric sensor.

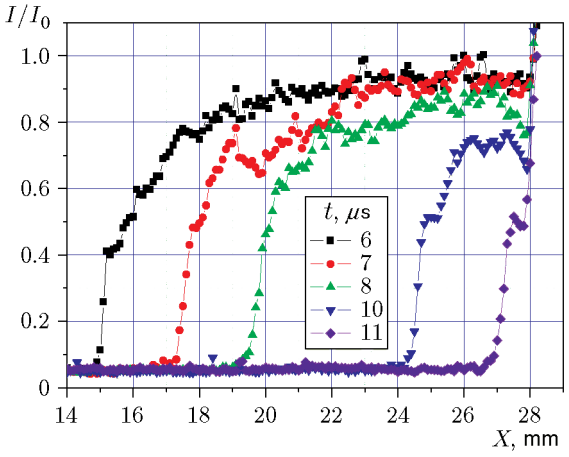

Fig. 9. Distributions of the normalized transmitted radiation at the time instants $t = 6$, 7, 8, 10, and 11 μs (the piezoelectric sensor is located at 28 mm from the FS).

DISCUSSION

The possibility of using SR for studying the flow of microparticles from large (more than 200 μm) roughness elements on a copper surface was described for the first time in [16]. Experimental data on a dust cloud ejected from shock-loaded lead with the roughness $Rz =$ 5–60 μm were reported in [14]. The x-ray pictures were taken along the grooves on the specimen surface (the specimen length was approximately 10 cm). The shapes of the mass distributions along the jet obtained in [14] coincide with the distributions of the present work. The use of SR generated by VEPP-3 allowed us to measure the mass distributions of the particle flow along its mo-

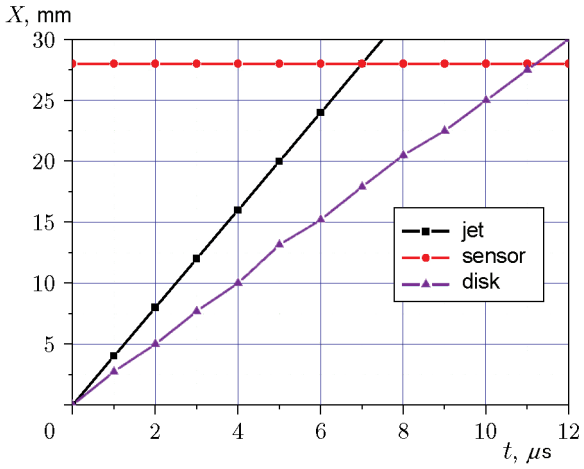

Fig. 10. Positions of the jet and FS (disk) in time.

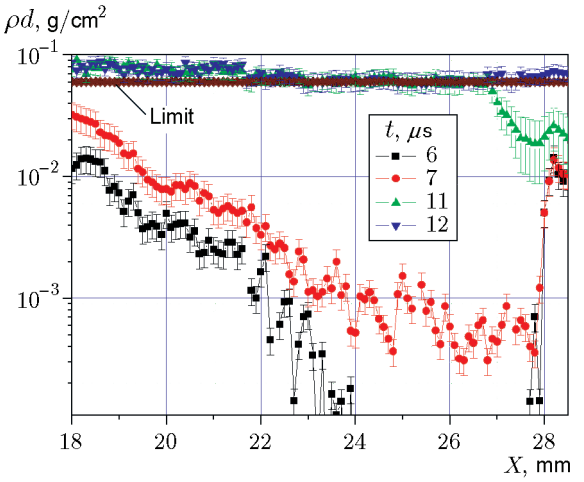

Fig. 11. Distributions of the specific mass of the jet before its impact onto the sensor at the time instants of 6, 7, 11, and 12 μs (the sensor is located at 28 mm from the FS).

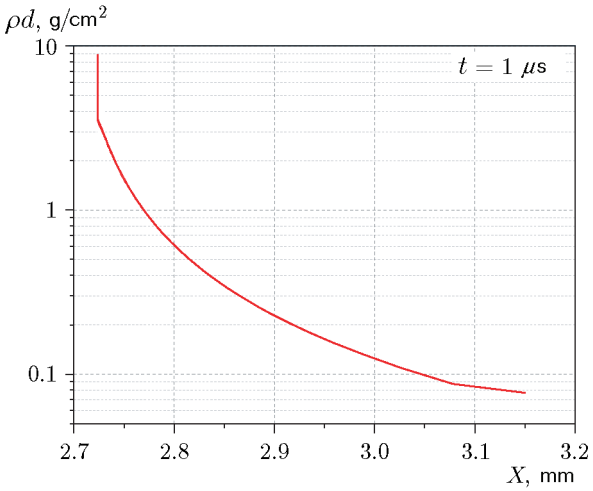

Fig. 12. Calculated distribution of the specific mass in the particle cloud at the time instant $t = 1$ μs.

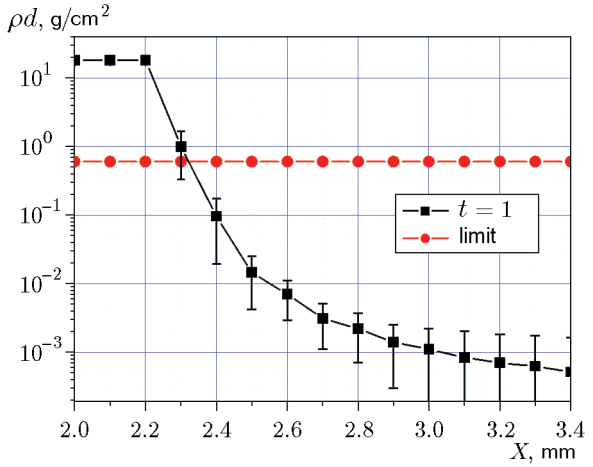

Fig. 13. Measured distribution of the specific mass on the SR beam in 1 μs after the beginning of FS motion.

tion within 5% up to the density of 1 mg/cm^3. The frame-by-frame photographs (see Fig. 7) of the particle flow reveal the deformations of the density distributions along the jet at different times ($t = 1$, 2, and 3 μs). The PDV measurement of the jet head velocity [9, 10] shows that it decreases after the first 2–4 μs. In accordance with our measurements (see Figs. 6 and 10), the jet velocity is almost constant.

The mathematical modeling of the particle ejection process was performed at the Institute of Experimental Physics. The calculations included the shock wave profile in the specimen, the FS velocity (2.72 km/s), and the velocity of the particle cloud front in vacuum (3.25 km/s). The measured values of the FS velocity coincide with the numerical predictions; the jet velocity (3.8 km/s) turned out to be slightly greater than the predicted value (3.25 km/s). A possible reason for this difference is the fact that the computations were performed for $Rz = 50$ μm, whereas the experiments were performed for $Rz = 60$ μm.

The calculated mass distribution is shown in Fig. 12; it agrees well with the measured distribution (Fig. 13). The predicted total ejected mass (8.55 mg/cm^2 [22]) is slightly greater than the measured value (5.6 mg/cm^2). This difference can be attributed to the curved shape of the frontal surface of the dust cloud.

Figure 14 shows the mass distributions measured by the piezoelectric sensor and SR detector. These distributions almost coincide in the interval from

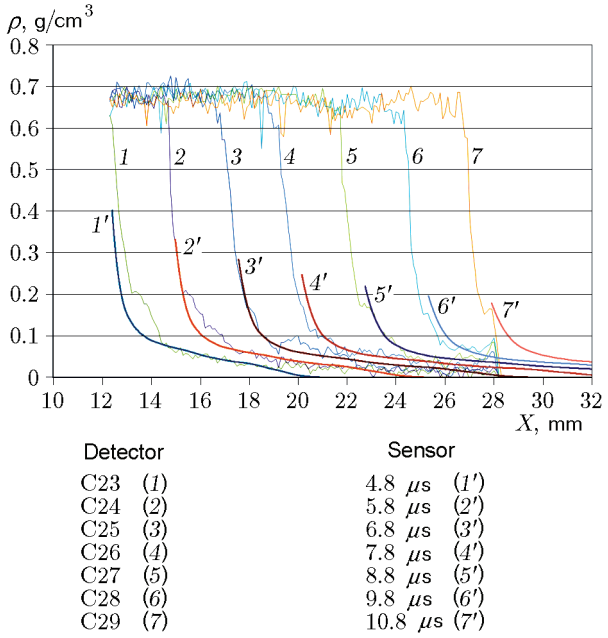

Fig. 14. Comparison of the specific densities of the jet measured by the piezoelectric sensor and SR detector.

0.02 to 0.2 g/cm^3. This fact confirms the validity of the assumption of self-similarity of motion of microparticle flows in vacuum, which is used in the piezoelectric method [12]. Based on the data of Fig. 13, one can more exactly calculate the momentum of particles imparted to the piezoelectric sensor. The resultant density distributions allow more precise calibration of the piezoelectric sensor readings and, thus, more accurate measurements of the mass and momentum of the particle flow in a wider range.

To increase the measurement accuracy, it is possible to increase the frame frequency of the detector (the VEPP-3 collider can generate SR pulses in 124 ns) and take pictures from different directions. The higher SR intensity also allows one to measure small-angle scattering on dust particles, which was demonstrated in [17].

CONCLUSIONS

Experiments on simultaneous registration of the microparticle flow position and density distribution with the use of synchrotron radiation and piezoelectric sensors are performed.

1. The distribution of the specific mass along the flow of microparticles with a specific mass from 1 mg/cm^2 is recorded. The distribution is nonuniform, but is consistent on the average with the calculations performed at the Institute of Experimental Physics.

2. The positions of the free surface and jet are measured as functions of time; the dynamics of their velocities is obtained.

3. The distributions of the specific mass along the jet before the impact onto the piezoelectric sensor are obtained. The piezoelectric sensors can be calibrated at extremely low density of microparticle flows.

This work was supported by the Russian Foundation for Basic Research (Grant No. 16-29-01050).

REFERENCES

1. A. L. Mikhailov, V. L. Ogorodnikov, V. S. Sasik, et al., "Experimental and Numerical Modeling of Particle Ejection from a Shock-Loaded Surface," Zh. Eksp. Teor. Fiz. **145** (5), 892–905 (2014).
2. V. A. Ogorodnikov, A. G. Ivanov, A. L. Mikhailov, et al., "Particle Ejection from the Shocked Free Surface of Metals and Diagnostic Methods for these Particles," Fiz. Goreniya Vzryva **34** (6), 103–107 (1998) [Combust., Expl., Shock Waves **34** (6), 696–700 (1998)].
3. A. L. Mikhailov, V. A. Ogorodnikov, V. S. Sasik, et al., "Experimental Study of Particle Ejection from a Shock-Loaded Surface," in *Proc. XV Khariton Scientific Readings* (VNIIEF, Sarov, 2013), p. 564.
4. V. A. Ogorodnikov, A. L. MIkhailov, V. V. Burtsev, et al., "Registration of Particle Ejection from the Free Surface of Shock-Loaded Specimens," Zh. Eksp. Teor. Fiz. **136** (3(9)), 615–620 (2009).
5. L. Signor, E. Lescoute, D. Loison, et al., "Experimental Study of Dynamic Fragmentation of Shock-Loaded Metals below and above Melting," EPJ Web Conf. **6**, 39012 (2010).
6. T. de Rességuier, D. Loison, E. Lescoute, et al., "Dynamic Fragmentation of Laser Shock-Melted Metals: Some Experimental Advances," J. Theor. Appl. Mech. **48** (4), 957–972 (2010).
7. M. B. Zellner, G. Dimonte, T. C. Germann, et al., "Influence of Shock Wave Profile on Ejecta," J. Appl. Phys. **101**, 063547 (2007).
8. M. B. Zellner, M. Byers, J. E. Hammerberg, et al., "Influence of Shock Wave Profile on Ejection of Micron-Scale Material from Shocked Sn Surfaces: An Experimental Study," in *Proc. of Dynamic Materials Conf., Brussels, Belgium, 2009.*
9. A. V. Fedorov, A. L. Mikhailov, S. A. Finyushin, et al., "Recording the Particle Velocity Spectrum at the Time the Shock Wave Reaches the Surface of Liquids of Different Viscosities," Fiz. Goreniya Vzryva **52** (4), 122–128 (2016) [Combust., Expl., Shock Waves **52** (4), 482–487 (2016)].

10. A. V. Fedorov, A. L. Mikhailov, L. K. Antonyuk, and I. V. Shmelev, "Experimental Study of the Stripping Breakup of Droplets and Jets after their Ejection from a Liquid Surface," Fiz. Goreniya Vzryva **52** (4), 115–121 (2016) [Combust., Expl., Shock Waves **52** (4), 476–481 (2016)].
11. D. S. Sorenson, P. Pazuchanics, R. Johnson, et al., "Ejecta Particle-Size Measurements in Vacuum and Helium Gas Using Ultraviolet In-Line Fraunhofer Holography," Report No. LA-UR-14-24722 (Los Alamos. Natl. Lab., 2014).
12. M. V. Antipov, I. V. Yurtov, A. A. Utenkov, et al., "Application of the Piezoelectric Method for Measuring the Parameters of Shock-Induced Dusty Flows," in *Proc. XIX KharitonScientific Readings* (VNIIEF, Sarov, 2017).
13. W. S. Vogan, W. W. Anderson, M. Grover, et al., "Piezoelectric Characterization of Ejecta from Shocked Tin Surfaces," J. Appl. Phys. **98**, 113508 (2005).
14. M. V. Antipov, A. B. Georgievskaya, V. V. Igonin, et al., "Results of Studying Particle Ejection from the Free Surface of Metals under the Shock Wave Action," in *Proc. XVII Khariton Scientific Readings* (VNIIEF, Sarov, 2015), p. 702.
15. W. T. Buttler, D. M. Oro, D. L. Preston, et al., "The Study of High-Speed Surface Dynamics Using a Pulsed Proton Beam," in *AIP Conf. Proc. on the Shock Compression of Condensed Matter*, Report No. LA-UR-2011-04269 (Los Alamos Natl. Lab., 2011).
16. K. A. Ten, E. R. Pruuel, A. O. Kashkarov, et al., "Detection of Microparticles in Dynamic Processes," J. Phys.: Conf. Ser. **774** (1), 012070 (2016).
17. K. A. Ten, E. R. Pruuel, A. O. Kashkarov, et al., "Synchrotron Radiation Methods for Registration of Particles Ejected from Free Surface of Shock-Loaded Metals," Phys. Procedia **84**, 366–373 (2016).
18. K. J. Ramos, B. J. Jensen, A. J. Iverson, et al., "In Situ Investigation of the Dynamic Response of Energetic Materials Using IMPULSE at the Advanced Photon Source," J. Phys.: Conf. Ser. **500**, 142028 (2014).
19. N. A. Popov, V. A. Shcherbakov, V. N. Mineev, et al., "On Thermonuclear Fusion during a Spherical Charge Explosion (Problem of Gas-Dynamic Thermonuclear Fusion)," Usp. Fiz. Nauk **178** (10), 1087–1094 (2008).
20. M. V. Astashkin, V. K. Baranov, A. B. Georgievskaya, et al., "Instability of the Free Boundary of a Water Layer Accelerated by the Taylor Wave," Pis'ma Zh. Eksp. Teor. Fiz. **99** (3), 146–148 (2014).
21. S. V. Mikhailov, A. S. Tyapin, B. S. Serov, and V. V. Rudenko, "Kinetic Model of Spalling Fracture of Materials under the Conditions of a High-Intensity Shock-Wave Action," in *Proc. XV Khariton Scientific Readings* (VNIIEF Sarov, 2013), p. 420.
22. A. B. Georgievskaya and V. A. Raevskii, "Effect of the Shock Wave Profile on the Size Distribution of Particles Ejected from the Free Surface of Metals under the Shock Wave Action (Numerical and Theoretical Study)," in *Proc. XVII Khariton Scientific Readings* (VNIIEF Sarov, 2015), p. 709.
23. M. V. Antipov, A. B. Georgievskaya, V. V. Igonin, et al., "Numerical MOdeling of Particle Ejection from a Shock-Loaded Surface," in *Proc. XV Khariton Scientific Readings* (VNIIEF, Sarov, 2013), p. 666.
24. K. V. Bandurkin, V. G. Kamenev, G. V. Kaplyukov, et al., "Experimental (Laser Interferometry Method, PDV) and Numerical Investigations of Motion of Disperse Phase Particles," Fiz.-Khim. Kinet. Gaz. Din. **16** (4), 1–14 (2015).
25. V. V. Mokhova, A. L. Mikhailov, A. V. Til'kunov, et al., "Mechanisms of Fracture of the Free Surface of Shock-Compressed Metals," Zh. Eksp. Teor. Fiz. **148** (6), 1146–1154 (2015).
26. V. V. Mokhova, A. L. Mikhailov, A. V. Til'kunov, et al., "Fracture of the Free Surface of Shock-Compressed Metals with Artificial Grooves," in *Proc. XVII Khariton Scientific Readings* (VNIIEF, Sarov, 2015), p. 307.
27. B. A. Kullback, G. Terrones, M. O. Carrara, and M. R. Hajj, "Quantification of Ejecta from Shock Loaded Metal Surfaces," in *Proc. on Shock Compression Conf., Chicago, 2011.*
28. E. B. Levichev, "Status and Perspectives of VEPP-4 Complex (in Russian)," Phys. Part. Nuclei Lett. **XIII** (7), (2016).
29. E. R. Pruuel, K. A. Ten, B. P. Tolochko, et al., "Realization of Capabilities of Synchrotron Radiation in Detonation Investigations," Dokl. Akad. Nauk **448** (1), 38–42 (2013).
30. V. M. Titov, E. R. Pruuel, K. A. Ten, et al., "Experience of Using Synchrotron Radiation for Studying Detonation Processes," Fiz. Goreniya Vzryva **47** (6), 3–16 (2011) [Combust., Expl., Shock Waves **47** (6), 615–626 (2011)].
31. V. M. Aulchenko, A. E. Bondar, V. N. Kudryavtsev, et al., "GEM-Based Detectors for SR Imaging and Particle Tracking," J. Instrum. **7** (3), 1–18 (2012).
32. L. I. Shekhtman, V. M. Aulchenko, V. N. Kudryavtsev, et al., "Upgrade of the Detector for Imaging of Explosions," Phys. Procedia **84**, 189–196 (2016).